MethodsX 10 (2023) 102018

Contents lists available at ScienceDirect

MethodsX

journal homepage: www.elsevier.com/locate/mex

A protection method for multi-terminal HVDC system based on fuzzy approach

Upma Sahu [a], Anamika Yadav [a,*], Mohammad Pazoki [b]

[a] Department of Electrical Engineering, National Institue of Technology Raipur, Chhattisgarh, India
[b] School of Engineering, Damghan University, Damghan, Iran

ARTICLE INFO

Method name:
Fuzzy Inference System based method

Keywords:
Multi-terminal HVDC network
DC fault detection
Fault section identification
Faulty pole recognition
Fuzzy Inference system

ABSTRACT

This paper presents a Fuzzy Inference System (FIS)-based method to detect a fault, identify the faulty section, and recognize the faulty pole in the Voltage Source Converter (VSC)-based Multi-Terminal High Voltage Direct Current (MT-HVDC) system. The method uses only rectifier end measurements of voltage and current signals. To achieve complete protection of the MT-HVDC system, three separate frameworks of FIS modules have been developed. The FIS-1 detects the presence of fault in either AC or DC segments. The FIS-2 identifies the fault section and eventually, the FIS-3 recognizes the faulty pole. The proposed method provides a rapid fault detection and it does not require any communication media as it is based on the rectifier-end measurements only. The efficacy of the implemented FIS-based method is evaluated in an MT-HVDC system simulated in MATLAB environment.

Important highlights of this method are:-

- FIS-based method is deployed using simple if-then rules, therefore very easy to implement.
- Effortless means to exploit one end measurements of MTDC system in an environment accustomed to power engineer.
- Proposed method provides a rapid fault detection and it does not require any communication link.

Specifications Table

Subject Area:	Engineering Science
More specific subject area:	Electrical Engineering
Method name:	Fuzzy Inference System based method
Name and reference of original method:	U. Sahu and A. Yadav, "Fault detection in MTDC network utilizing one end measurements," 2019 8th Int. Conf. Power Syst. Transit. Towar. Sustain. Smart Flex. Grids, ICPS 2019, 2019.
Resource availability:	There are no special resources

Introduction

A key aspect answerable for getting tremendous care in the growth of traditional technology is growing demand for the electricity and hence growing the power transmission capacity of the transmission network. As a consequence of rising need for the electricity and the inclusion of renewable energy resources in power networks, multi-terminal HVDC (MT-HVDC) systems have become more

* Corresponding author.
E-mail addresses: ayadav.ele@nitrr.ac.in (A. Yadav), pazoki.m@du.ac.ir (M. Pazoki).

https://doi.org/10.1016/j.mex.2023.102018
Received 26 October 2022; Accepted 13 January 2023
Available online 14 January 2023

appealing in recent years [1]. In the literature survey, transmission network to transmit large amount of power over far distances has been addressed based on the Current Source Converter (CSC) [2]. However, as opposed to the MT-HVDC system with voltage source converter (VSC), the ability to expand the MT-HVDC system with CSC becomes comparatively more troublesome. Thereby, the enhancement to the MT-HVDC system of the established two-terminal transmission networks is not compelling for large-scale construction [3]. Compared with CSC-based HVDC systems, VSC-based HVDC systems improve the flexibility of power transmission network. In addition, less operational cost and redundant switching states will be provided in the VSC-based HVDC system [4,5]. Moreover, the VSC-based HVDC systems have overcome few of the drawbacks associated with Line Commutated Converter (LCC-based HVDC); for instance, the power electronics switches used in the VSC provide both turn-on and turn-off capability at desired instant as compared to the thyristors in the CSC which can provide only turn-on capability and turns off as per natural line commutation. Since VSC-based HVDC system offers a steady voltage, frequency, and phase angle for wind farms, it is a common technology for connecting integrated systems such as large-scale wind farms. Further, the VSC-based HVDC can easily start and incorporate the offshore wind farm into the grid, which is simpler than using LCC-based HVDC [2,6–8]. In the VSC, changing the direction of the DC current achieves the power flow reversal, whereas the DC voltage polarity in the LCC has to be inverted at all interconnected stations [2,7,8]. The use of VSC-based HVDC system enables the implementation of multi-terminal HVDC (MT-HVDC) grids [9,10]. One of the main benefits is the suitable approach to integrating VSC over various DC terminals for the MT-HVDC system. The recent growth in research makes it easy to incorporate the numerous VSC-based MT-HVDC systems into distributed energy resources [11–13]. Generally, compared with the CSC-based HVDC systems, the VSC-based MT-HVDC network is more suitable for various application mentioned in [14–16].

By prevailing literature survey, various fault detection, location and classification methods have been discussed. These are the decisive actions to obtain a reliable and correct operation [17–19]. The authors in [20] proposed an artificial neural network (ANN)-based fault detection method by applying harmonics of voltage waveform in rectifier side in the HVDC system. A novel method for detection of a fault and fault distance in the HVDC system using ANN is presented in [21]. Here, the ANN is used as a pattern recognizer to correlate post-fault DC voltage signal to fault distance. In [21], a fault location method in the HVDC system based on ANN is also described. A fault detection method based on the wavelet in the MT-HVDC system for combination of underground and overhead transmission lines are introduced in [22]. Such methodology preferred for finding the location of fault raises the calculative burden due to numerous constrictions, such as selection of mother wavelets, noisy conditions, and need for various sensors. In [23], three modules implemented based on fuzzy inference system (FIS) detect the faults, discriminate the fault section, and identifies the faulty pole for two-terminal HVDC systems. The method has not been tested for operation in a MT-HVDC system. The primary advantage of the MT-HVDC system relative to the HVDC transmission system is that there are many transmission lines between converter stations to shape mesh networks and maximize network stability, which increases the efficiency of the power supply, decreases the number of converter stations, and lowers maintenance and operational costs [24]. This FIS-based method senses a fault and identifies a defective segment within a short time, which clarifies the supremacy of the FIS-based method over other methods. In [25], a fault detection based on FIS in MT-HVDC system is proposed, but more consideration and fault classification tasks are not reported. In [32], a fault identification scheme in HVDC line based on the convolutional neural network (CNN), fast Fourier transform (FFT), and gramian angular field (GAF) is proposed. The scheme suffers from high computation complexity using three tools. In [33], an Intrinsic Time Decomposition-based scheme is designed to protect the a HVDC system. Finding the threshold value is a challenging issue in the proposed scheme in [33]. In [34], a fault identification scheme by using wavelet transform modulus maximum is proposed in a HVDC line. The scheme needs high sampling frequency to detect a fault.

In this paper, a method for detection of fault, section identification, and faulty pole recognition in the VSC-based MT-HVDC system is offered by using FIS.

This method is the extension of method proposed in [25] that extends the applicability of the FIS-based method to detect and classify all types of faults and identify the faulty pole in a MT-HVDC system considering different challenging cases. The MT-HVDC system is built by linking three VSCs to the network's various DC terminals. The numerous types of faults are generated over the DC transmission line at different locations. Easy rules for fault detection, section identification, and fault pole recognition are used in the proposed method, which decrease the technique's calculative burden and complication. Moreover, the proposed method will detect the fault in the minimum possible time for VSC-based MT-HVDC system.

The structure of the paper is as follows: Section-2 represents the design of sample system. Section-3 describes the proposed method by using FIS technique. Software simulation results are presented in Section 4. Section 5 compares with other approaches and the conclusion of overall paper is described in Section 6.

VSC-based MT-HVDC system

Fig. 1 displays three 200 MVA (+ /- 100 kV DC) VSCs in a MT-HVDC system. In the sample system, the length of the first transmission line (L 1), the second transmission line (L 2), and the third transmission line (L 3) are 200 km, 50 km, and 100 km, respectively [26]. Table 1 displays the parameters used in the simulation of the sample system. Pi section is used for modeling of transmission line along with the smoothing reactor of 8 mH in series. For the transfer of power between three equivalent 230 kV, 2000 MVA, 50 Hz rated AC systems, this transmission line will be used. In case of rectification as well as inversion, modeling of VSC converter is done using Neutral Point Clamped (NPC) topology. To achieve this, power electronic devices such as IGBT/ diodes are used and the three-level output voltage will be generated. To drive the power switches of the VSCs, sinusoidal pulse width modulation (SPWM) signals are applied to the gate terminal of the switches. The SPWM signal is produced based on comparing the reference fundamental frequency of signal, 50 Hz, with the 1350 Hz (27 × fundamental frequency) carrier signal. In the sample system, transformers (Yg- Δ), AC filters, converters, capacitor and DC filter are simulated. In order to dominate the higher order

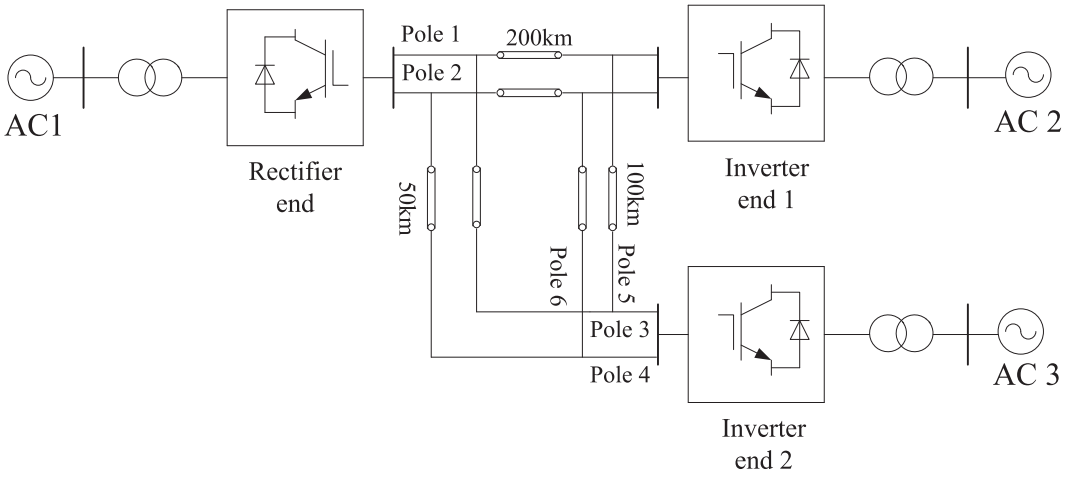

Fig. 1. The sample MT-HVDC system.

Table 1
MT-HVDC system parameters.

Parameters	Value
Source-1(Rectifier end)	230 kV,2000MVA,50Hz
Ac filter (capacitor banks)	40 MVAr
HVDC smoothing reactors	8 mH
High-order passive damped filters	$Q = 15$
Resistance (Ω/km)	0.015
Inductance (H/km)	0.792e-3
Capacitance (F/km)	14.4e-9
Rated power of three-phase transformer (Yg/Y/ Δ)	200e6 VA
Frequency	50 Hz
Voltage (pH-pH) of Winding 1	230e3 × 0.915
Voltage (pH-pH) of Winding 2	100e3
Voltage (pH-pH) of Winding 3	100e3
Per unit magnetization resistance	500
Per unit magnetization inductance	500
Source-2 and Source-3 (Inverter end)	230 kV, 2000 MVA, 50 Hz

harmonics (27th and 54th), the 40 MVAr high-pass shunt AC filter is used. The reactance of converter and the leakage reactance of transformer are 0.15 pu and 0.15 pu, respectively. They can control the active and reactive power corresponding to VSCs in a HVDC system. In the DC part of sample system, the ripple of voltage and strain of reactive power strain have been improved by using the high ratings of DC capacitors inserted in VSCs. Tunned high-frequency blocking filtering is used in the system to resolve the effect of most dominant 3rd order harmonics in the negative and positive half-side pole voltages. The sample system to study the performance of the proposed method is simulated by modifying the two-terminal HVDC system as shown in Fig. 1 [26,27]. The effectiveness of the proposed method is evaluated by using this sample system.

Method details

The FIS-based method is preferred in this paper to detect the fault, identify the fault section, and recognize the faulty pole because it is straightforward to implement and does not obligate a training module to generate outputs. The fuzzy method is taken due to less computational effort than other soft computing techniques.

Two significant categories of FIS exist: 1. Mamdani and 2. Sugeno. The fuzzy rules of Mamdani FIS are less than rules of Sugeno FIS and hence the proposed method is implemented by the Mamdani FIS [26]. The method focuses on the current magnitude of root mean square (RMS) captured during normal and abnormal conditions. The input of fuzzy modules are the logical variables which are based on the continues values corresponding to different analog parameters. Information on the various characteristics of erratic input signals can be easily interpreted by FIS from different perspectives. Three distinct processes in FIS can well examine the preceding reality: 1. fuzzification, 2. fuzzy inference, and 3. defuzzification.

The transformation from crisp (bivalued) input values into linguistic values is known as fuzzification step. A simple fuzzification algorithm is performed by maintaining μ_i constant and x_i is transferred to fuzzy set Q(x_i) representing the expression about x_i for a fuzzy set $A = \{\mu\_(i) \; |x\_(i) \; |x\_i \; \epsilon X\}$. The fuzzy set Q(x_i) is titled the kernel fuzzification. It can be represented as the fuzzified set

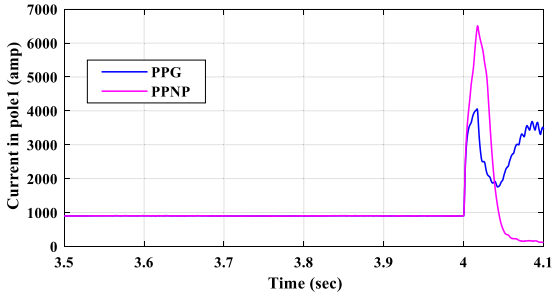

Fig. 2. The fault current of pole-to-ground fault and pole-to-pole short circuit fault.

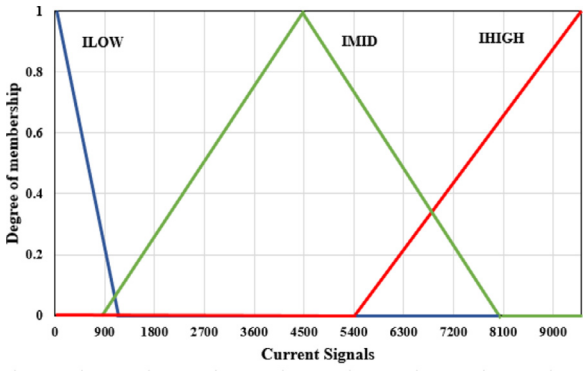

Fig. 3. Degree of membership function (i.e., ILOW (Low), IMID (Medium), and IHIGH (High)) for fault detection.

$\underset{\sim}{A} = \mu\_1\ Q(x\_1) + \mu\_2\ Q(x\_2) + \cdots + \mu\_n\ Q(x\_n)$. The symbol ~ corresponds to fuzzified and the above fuzzification mode is considered support fuzzification (s-fuzzification). There is further fuzzification approach named grade fuzzification (g-fuzzification) where x_i has been held constant and μ_i has been represented as a fuzzy set and fuzzification is carried out using these techniques. In the structure of FIS, first step is fuzzification. Fuzzification is a step in deciding the degree to which the input data belongs through the membership functions to each of the relevant fuzzy sets. The knowledge base comprises the information unique to the application domain. Collectively, the rule base and the data base are considered as the knowledge base. Accordingly, the decision-making unit performs operation based on these rules. The resulting membership functions are formed in this approach by considering the union of the output of each rule, which implies that the overlapping region of the fuzzy output collection is counted as one, giving further outcome. The FIS working system is based on the FIS decision-making rules that are specified in terms of the "IF … THEN" statement and are associated with the aid of "OR"/"AND" connectors. Finally, defuzzification is the transfer of the output fuzzy set to a precise output value.

Fuzzy module for detection of fault (FIS-1)

Positive- or negative-pole-to-ground fault (PPG or NPG) and Positive- and negative-pole-to-pole fault (PPP or NPP) as two main types of faults may happen in the in the HVDC transmission line. The voltage and current of the system will change tremendously if a fault occurs on the transmission network. The magnitude of the DC voltage signal will reduce and an abrupt upsurge in the DC current signal will appear. The magnitude of the pole-to-pole short-circuit fault is more enormous than that of the pole-to-ground fault [28], as demonstrated in Fig. 2. If the fault is not identified and reported at the least possible moment, this can lead the complete cessation of the system. A triangular membership feature is developed by the proposed Mamdani FIS system as it is well suited for suggested fault detection purposes using the trial-and-error method. In the fault detection module of the proposed method, the analog input is the DC current signal and it is fuzzified for different ranges utilizing the triangular membership function: 1. Low, 2. Medium, and 3. High as drawn in Fig. 3. Magnitude of the DC current signal during the pre- and post-fault in the MT-HVDC network sets the membership positions. To frame the fuzzy rules for fault detection, the rms value of dc current in each pole at rectifier end is measured for fault with zero fault resistance and high fault resistance to envisage the maximum and minimum value of current during fault situation. And the lower, middle and upper limit of the current is identified. And then if rms value of current is in low or medium range then it is considered as non-faulty situations while if rms value of current in a particular pole is high, then only it is recognized as faulty pole, then it is considered as faulty situation, otherwise it is healthy. The output of FIS-1 is a binary signal, i.e. output= 0 for no-fault condition and output=1 for occurrence a fault in both AC or DC section.

The fuzzy rules have been formed based on Table 2 for fault detection purpose.

Table 2
Fuzzy rules of FIS-1.

Input current	Output	Recognition of fault
ILOW	0	No-Fault
IMID	1	Faulty Condition
IHIGH	1	Faulty Condition

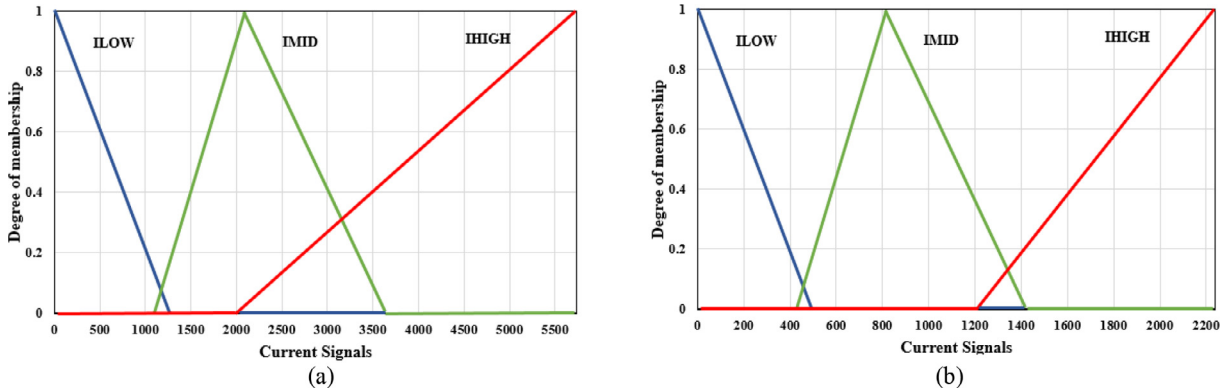

Fig. 4. Degree of membership function (a) input 1 or section 1 for fault section identification (b) input 2 for section 2 for fault section identification.

Table 3
Fuzzy rules of FIS-2.

Input current in DC section-1(S1)	Input current in AC section-2 (S2)	Fault in DC line side (S1)	Fault in AC side (S2)	No faults TN (0)
ILOW	ILOW	0	0	1
ILOW	IMID	0	0	1
ILOW	IHIGH	0	1	0
IMID	ILOW	0	0	1
IMID	IMID	0	0	1
IMID	IHIGH	0	1	0
IHIGH	ILOW	1	0	0
IHIGH	IMID	1	0	0
IHIGH	IHIGH	1	0	0

Fuzzy module for fault section identification (FIS-2)

The module of fault section identification in the proposed method is implemented in the FIS-2. The DC current signal and the AC current (RMS) signal from the rectifier ends are used as input for the module of fault section identification. The output of FIS-2 is a binary signal, 0 or 1, i.e. output= 0 for no-fault condition and output=1 for DC section (S1) and AC section (S2). Considering the magnitude of DC current signals, three sets of occupied membership function are implemented as shown in Fig. 4. Rules for the module of fault section identification (FIS-2) are given in Table 3. To fuzzify the input variable as depicted in Fig. 4 and also to frame the fuzzy rules for fault section identification, the rms value of dc current in each pole and ac current at rectifier end is measured during fault with zero fault resistance and high fault resistance to determine the maximum and minimum value of fault current. Thereafter the lower, middle and upper limit of the current is identified. And then if current is in low or medium range then it is considered as non-faulty situations while if ac/dc current is in high range then it is considered as faulty situation and corresponding ac or dc section is recognized as faulty respectively.

Fuzzy module for faulty pole recognition (FIS-3)

In this module, the DC current signals corresponding to both poles at the rectifier ends is taken as input for the design of the FIS-3 module for the faulty pole recognition. Considering the magnitude of DC current signals of both poles, three sets of occupied membership function are implemented as shown in Fig. 5. If rms value of a particular pole is high, then only it is recognized as faulty pole, otherwise it is healthy. The output of the FIS-based faulty pole recognition results in either 0 or 1. The output of FIS-3 is a binary signal, i.e. output= 0 for non-fault poles and output=1 for faulty poles. Rules are given in Table 4 for the module of faulty pole recognition (FIS-3).

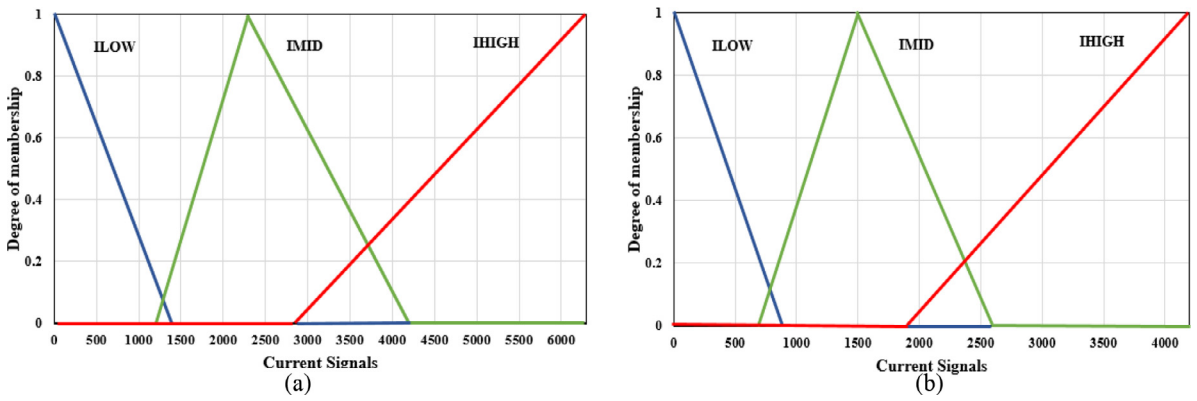

Fig. 5. Degree of membership function (a) Input of pole 1 for faulty pole recognition (b) Input of pole 2 for faulty pole recognition.

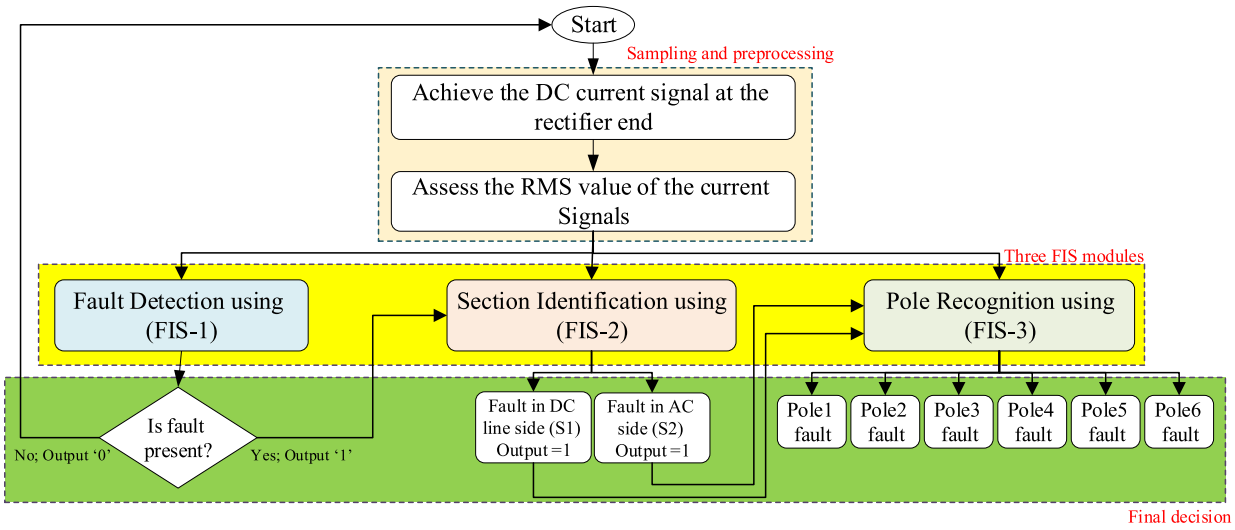

Fig. 6. Flowchart of the proposed method.

Table 4
Fuzzy rules of FIS-3.

Rules	Input current in poles		Trip Logic output of the strategy based on FIS		Ascertained Faulty Poles
	Pole 1	Pole 2	Pole 1	Pole 2	
Rule 1	IHIGH	ILOW	1	0	Fault in Pole 1
Rule 2	ILOW	IHIGH	0	1	Fault in Pole2
Rule 3	ILOW	ILOW	0	0	No fault
	Pole 3	Pole 4	Pole 3	Pole 4	
Rule 4	IHIGH	ILOW	1	0	Fault in Pole 3
Rule 5	ILOW	IHIGH	0	1	Fault in Pole 4
Rule 6	ILOW	ILOW	0	0	No fault
	Pole 5	Pole 6	Pole 5	Pole 6	
Rule 7	IHIGH	ILOW	1	0	Fault in Pole 5
Rule 8	ILOW	IHIGH	0	1	Fault in Pole 6
Rule 9	ILOW	ILOW	0	0	No fault

The general overview of the proposed method is illustrated in Fig. 6 after designing three FIS modules. The Pseudo code for the Fuzzy Inference System is also illustrated herein. The FIS is adapted for fault detection, fault section identification, and faulty pole recognition in the VSC-based MT-HVDC system. The method is competent to detect, identify, and analyze all fault types at different locations.

Pseudo code for the Fuzzy Inference System
Begin
Selecting Input Variable:
Select dc current signal measured at one end of the pole 1 to 6 as input
Preprocessing:
Determine the RMS value of the input current signals
Fuzzification:
Transform crisp input into truth values by input membership functions
Fuzzy rules based on expert knowledge:
Determining set-1 of fuzzy rules for fault detection
Determining set-2 of fuzzy rules for section identification
Determining set-3 of fuzzy rules for pole recognition
Rule evaluation:
Establish the rule strength by combining the fuzzified inputs based on fuzzy rules
Find the consequent of the rule by combining the rule strength and the output membership function
Combine all the consequents to get distribution of output
Defuzzification:
Defuzzification of output distribution to provide precise output value
End

Method results

The performance of the proposed method is evaluated against different fault parameters such as fault location, fault resistance, signal-to-noise ratio (SNR) values, transmission line parameters, near-end faults, far-end faults, and power angle. Decrease of DC voltage, increase of rectifier current, and fall to zero of inverter current are the consequences of a fault happening. The simulated current waveforms for pole-to-ground fault at the rectifier side corresponding to pole 1 and pole 2 are shown in Fig. 7(a). Further, faulty pole recognition is indicated in Fig. 7(b) where the fault occurs at time $t = 4$ s and the faulty pole is recognized at 4.00493 s. It should be noted that the output of pole 1 is 1 and the output of pole 2 is 0 which indicate the faulty pole is pole 1 during pole 1-to-ground (P1G) fault at 5 km with fault resistance of 1 Ω. Similarly, the simulated current waveforms for P1G fault at the rectifier side for section 1 and section 2 are represented in Fig. 8(a) and (b). The performance of the fault section identification module is shown in Fig. 8(a) and (d) where the fault occurs at time $t = 4$ s and the fault section is identified at 4.00319 s. As shown in the

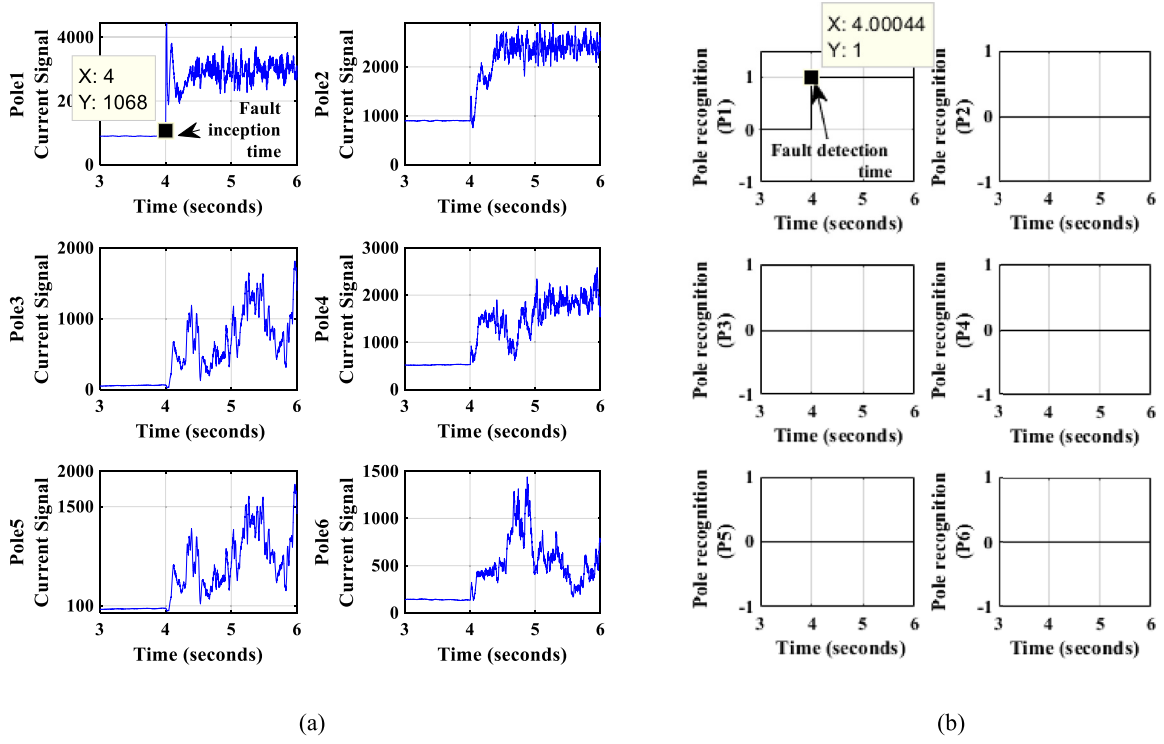

Fig. 7. (a) Current signal at poles and (b) Recognition outputs of pole during P1G fault at 5 km with fault resistance of 1 Ω.

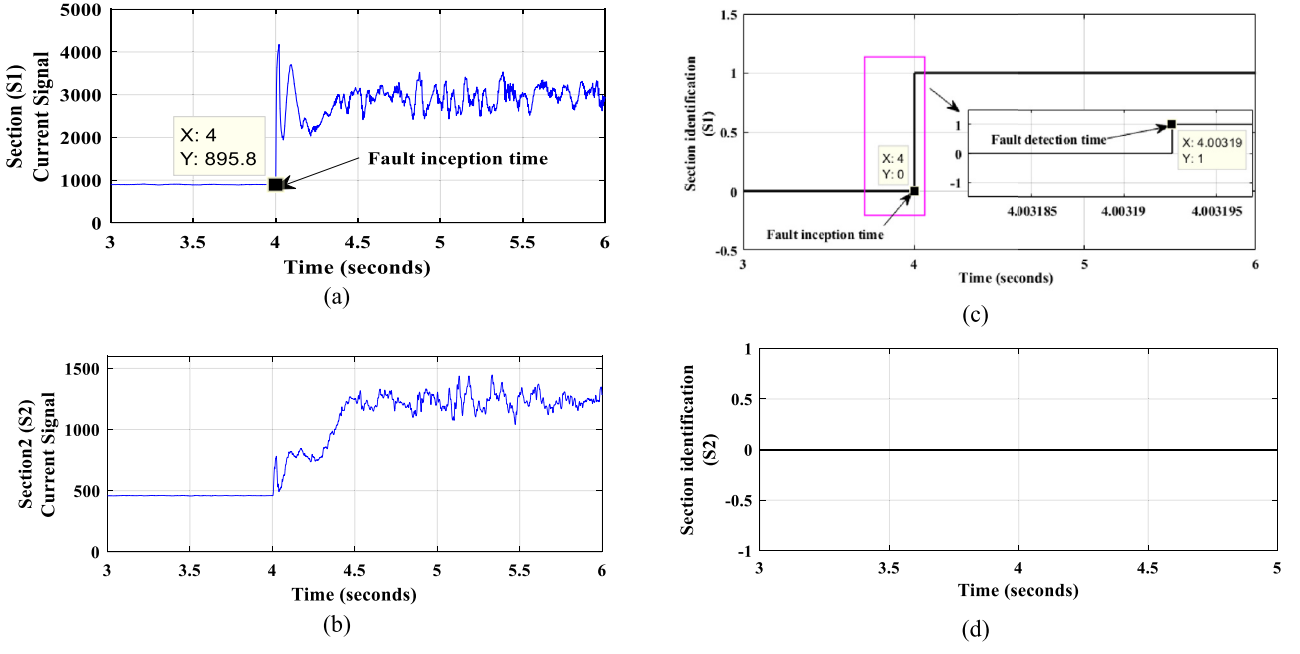

Fig. 8. (a) The current signal of DC section (S1), (b) The current signal of AC section (S2), (c) Output signal of FIS-2 for DC section (S1), and (d) Output signal of FIS-2 for section (S2) during P1G fault (fault resistance=1 Ω).

Table 5
Results obtained by the proposed method against different fault types and fault resistances.

Fault type	Fault Resistance (Ω)	Fault detection		Section identification				Identification Result
		Trip logic output	Detection Time (ms)	Section 1		Section 2		
				Trip logic output	Identification Time (ms)	Trip logic output	Identification Time (ms)	
PP1G	1	1	0.44	1	3.19	0	–	Fault in DC side (S1)
	20	1	0.51	1	3.2	0	–	Fault in DC side (S1)
	40	1	0.68	1	3.81	0	–	Fault in DC side (S1)
	60	1	0.69	1	3.71	0	–	Fault in DC side (S1)
NP2G	1	1	0.41	1	3.67	0	–	Fault in DC side (S1)
	20	1	0.50	1	4.76	0	–	Fault in DC side (S1)
	40	1	0.59	1	3.76	0	–	Fault in DC side (S1)
	60	1	0.68	1	3.31	0	–	Fault in DC side (S1)
PP3G	1	1	0.26	1	3.48	0	–	Fault in DC side (S1)
	20	1	0.35	1	3.68	0	–	Fault in DC side (S1)
	40	1	0.44	1	4.78	0	–	Fault in DC side (S1)
	60	1	0.53	1	3.45	0	–	Fault in DC side (S1)
NP4G	1	1	0.34	1	3.97	0	–	Fault in DC side (S1)
	20	1	0.49	1	3.32	0	–	Fault in DC side (S1)
	40	1	0.46	1	3.56	0	–	Fault in DC side (S1)
	60	1	0.57	1	4.42	0	–	Fault in DC side (S1)
PP5G	1	1	0.38	1	3.65	0	–	Fault in DC side (S1)
	20	1	0.47	1	3.76	0	–	Fault in DC side (S1)
	40	1	0.63	1	4.41	0	–	Fault in DC side (S1)
	60	1	0.68	1	5.67	0	–	Fault in DC side (S1)
NP6G	1	1	0.37	1	3.38	0	–	Fault in DC side (S1)
	20	1	0.57	1	4.64	0	–	Fault in DC side (S1)
	40	1	0.63	1	5.67	0	–	Fault in DC side (S1)
	60	1	0.67	1	5.73	0	–	Fault in DC side (S1)
PP1NP2	1	1	0.42	1	3.32	0	–	Fault in DC side (S1)
	5	1	0.57	1	4.56	0	–	Fault in DC side (S1)
	10	1	0.59	1	5.76	0	–	Fault in DC side (S1)
	15	1	0.69	1	5.87	0	–	Fault in DC side (S1)
PP3NP4	1	1	0.47	1	3.35	0	–	Fault in DC side (S1)
	5	1	0.64	1	4.56	0	–	Fault in DC side (S1)
	10	1	0.59	1	5.67	0	–	Fault in DC side (S1)
	15	1	0.63	1	5.87	0	–	Fault in DC side (S1)
PP5NP6	1	1	0.45	1	3.78	0	–	Fault in DC side (S1)
	5	1	0.56	1	4.67	0	–	Fault in DC side (S1)
	10	1	0.68	1	5.65	0	–	Fault in DC side (S1)
	15	1	0.75	1	5.34	0	–	Fault in DC side (S1)
F1	1	1	3.34	0	–	1	5.67	Fault in AC side (S2)
F2	1	1	3.56	0	–	1	5.97	Fault in AC side (S2)
F3	1	1	4.67	0	–	1	5.76	Fault in AC side (S2)

figure, the output of the DC section 'S1′ is 1 and the output of the AC section 'S2′ is 0. Results obtained from the fault occurring in DC section with different fault resistances are listed in Table 5.

Performance of the method against varying fault resistance

The effect of varying fault resistance is taken into the discussion since the fault resistance affects the fault analysis. Therefore, the proposed method is tested against varying fault resistance. When the value of fault resistance increases, the magnitude of the current signal decreases. Fig. 9(a) represents the current waveform when resistance is varied from 0 to 100 Ω in a stage of 20 Ω and Fig. 9(b) shows the corresponding output of fault detection by the proposed method during PP1G fault at 5 km. Based on the simulation results, changing the fault resistance, increases the detection time which are shown in Table 5. The proposed method detects the fault and identifies the fault sections in a short time. Thus, the proposed method is not affected against change of fault resistance parameter significantly.

Performance of the method against near-end faults

The proposed method is tested at different fault locations from 3 km to 8 km with various types of near-end faults and the results tested are mentioned in Table 6. The simulated current waveforms during P1G fault at 4 km from the end-bus of the rectifier are shown in Fig. 10(a). Accordingly, Fig. 10(b) shows the output trip signal issued by the proposed detection module after occurring a near-end fault. It can be observed that the fault occurs at time $t = 4$ s and the fault is detected at 4.00041 s. After occurring a fault at

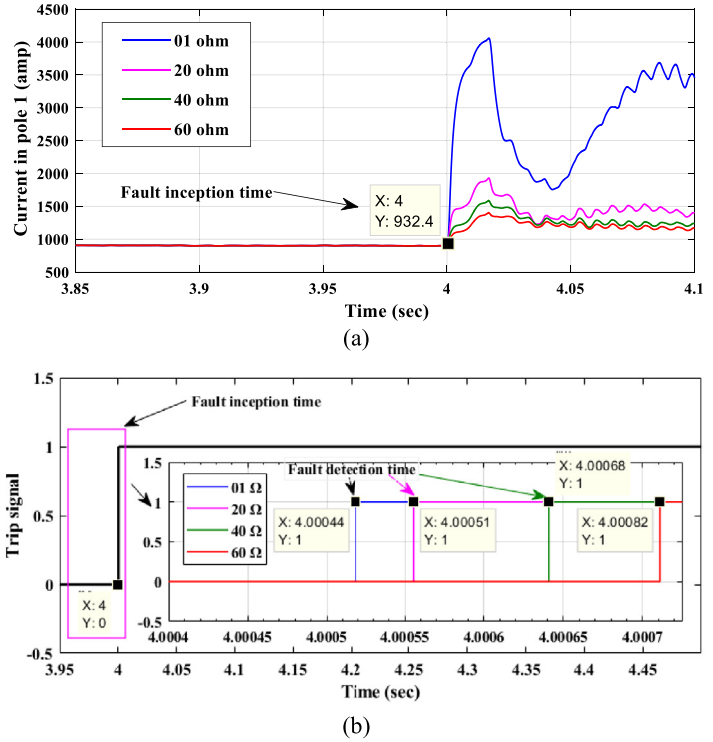

Fig. 9. (a) Variation of fault resistance and (b) Output of fault detection module.

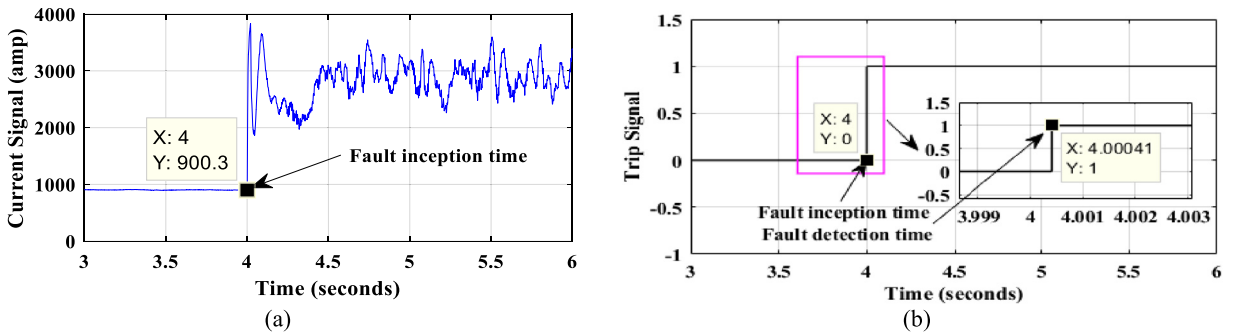

Fig. 10. (a) The simulated DC current signal corresponding to near-end fault at 4 km and (b) Output signal of FIS-1 during P1G fault at 4 km.

Table 6
Performance of the proposed method against near-end faults.

Fault Location (Near-End) in km	Fault Detection		Section Identification				Identification Result
	Trip logic output	Detection Time (ms)	Section 1		Section 2		
			Trip logic output	Identification Time (ms)	Trip logic output	Identification Time (ms)	
3	1	0.37	1	2.98	0	–	Fault in DC side (S1)
4	1	0.41	1	3.11	0	–	Fault in DC side (S1)
5	1	0.43	1	3.19	0	–	Fault in DC side (S1)
6	1	0.46	1	3.43	0	–	Fault in DC side (S1)
7	1	0.49	1	3.47	0	–	Fault in DC side (S1)
8	1	0.52	1	3.51	0	–	Fault in DC side (S1)

Table 7
Performance of the proposed method against far-end faults.

Fault Location (Far-End) in km	Fault Detection		Section Identification				Identification Result
	Trip logic output	Detection Time (ms)	Section 1		Section 2		
			Trip logic output	Identification Time (ms)	Trip logic output	Identification Time (ms)	
193	1	1.9	1	4	0	–	Fault in DC side (S1)
194	1	1.81	1	4.67	0	–	Fault in DC side (S1)
195	1	1.75	1	4.87	0	–	Fault in DC side (S1)
196	1	1.68	1	5.56	0	–	Fault in DC side (S1)
197	1	1.65	1	5.87	0	–	Fault in DC side (S1)
198	1	1.58	1	5.93	0	–	Fault in DC side (S1)
199	1	1.57	1	6.32	0	–	Fault in DC side (S1)
200	1	1.57	1	6.34	0	–	Fault in DC side (S1)

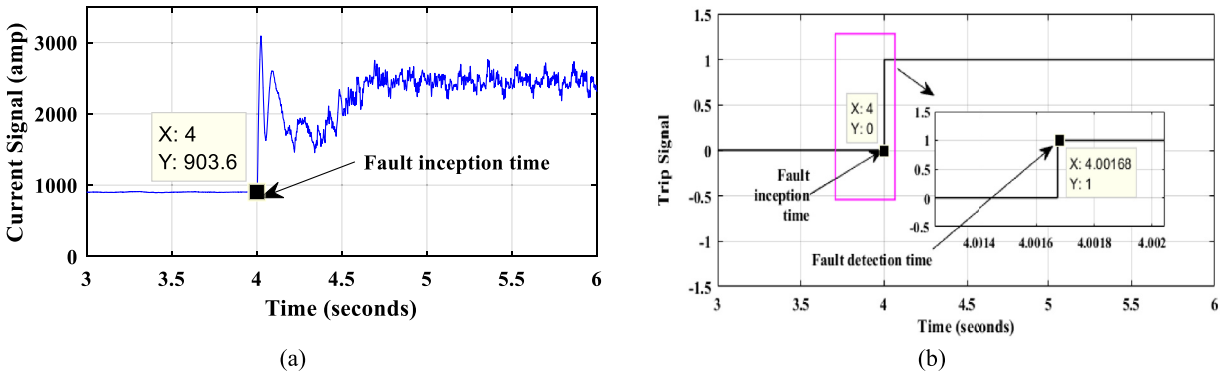

Fig. 11. (a) The simulated DC current signal corresponding to far-end fault at 196 km and (b) Output signal of FIS-1 during P1G fault at 196 km.

the rectifier side, the magnitude of the DC current signal significantly increases. This abrupt diversification feature of the DC current signal is employed to detect the fault. The proposed method needs short time to detect the fault and identify the section. Therefore, the proposed method identifies the faulted section in an effective manner.

Performance of the method against far-end faults

The proposed method is evaluated against far-end faults at a distance of 196 km to 200 km, and the results are listed in Table 7. The simulated current waveforms for P1G fault happened at 196 km from the end-bus of the rectifier are illustrated in Fig. 11(a) and (b) represents the output of fault detection module. Compared to near-end faults, the magnitude of the fault current is comparatively less in the case of a far-end fault. Even though the proposed method correctly detects the far end faults. Furthermore, as shown in Table 7, the proposed method detects the fault and identifies the section in an appropriate time.

Performance of the method against varying power angle

The proposed method is assessed at the rectifier end with differing power angles (5° −15°). Moreover, fault scenarios are evaluated at the AC side of the sample system with the value of fault resistance 1 Ω. Power system stability is an important issue for a secure system operation. Fig. 12(a)-(e) depicts the simulation tests of a pole-to-ground fault at the rectifier side during fault (phase A-to-ground fault) in AC section with varying power angle (5°) and fault resistance of 1 Ω. Fig. 12(a) and (c) depicts the current signals of section 1 (S1) and section (S2), respectively. Fig. 12(b) shows the output signal of the FIS-1 and Fig. 12(d) and (e) indicates the result of the FIS-2. As the fault occurred in the section 2 (S2) i.e. in the AC side, the output signal of FIS-2 corresponding to the section 1 (S1) is 0 (no-fault condition) and the output signal of FIS-2 corresponding to the section 2 (S2) is 1 (faulty condition) as shown in Fig. 12(d)-(e). Table 8 illustrates the results of the proposed method against change the load angle. Moreover, the method is able to detect all types of faults and identify the section of the fault in both the rectifier and the inverter ends.

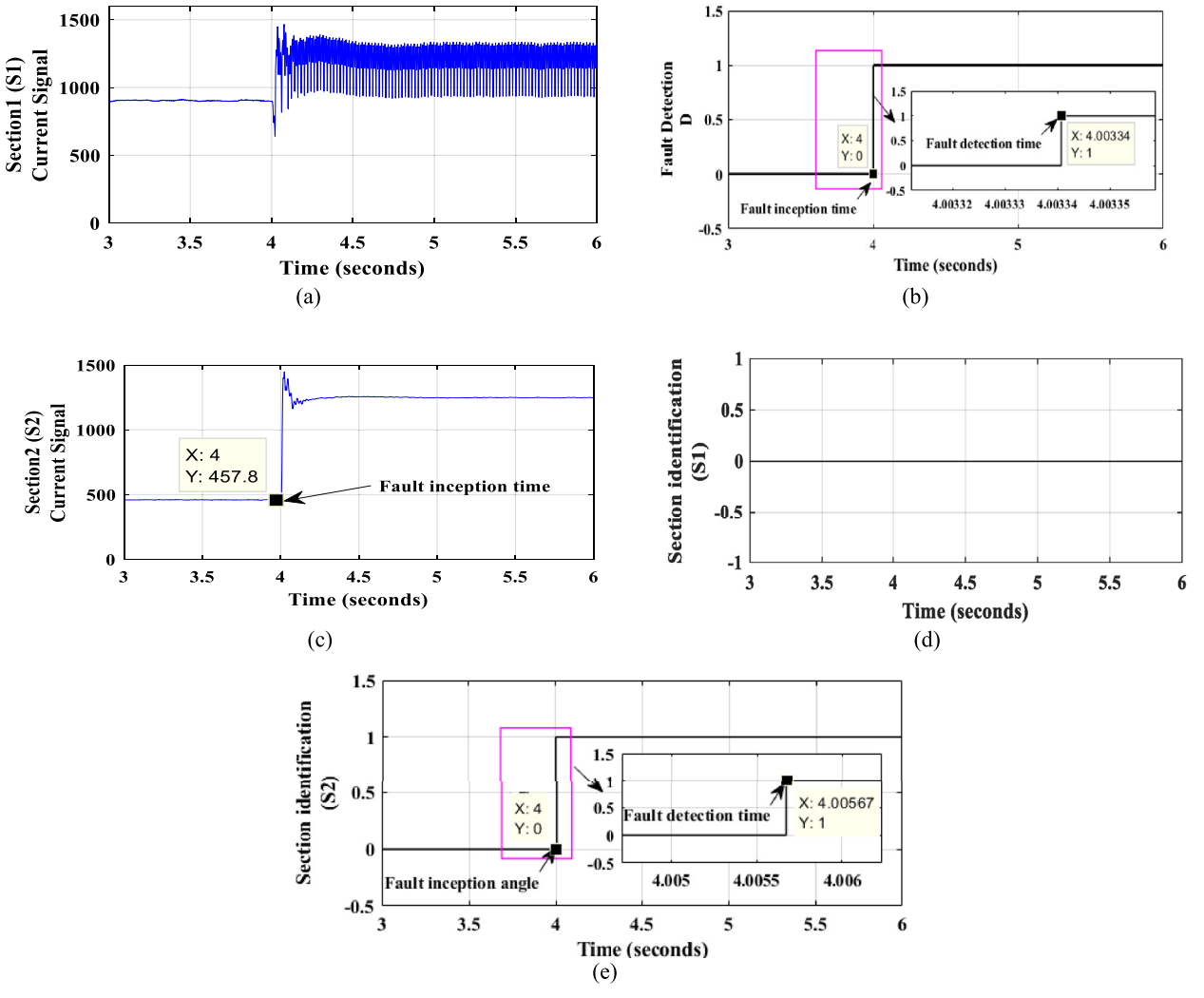

Fig. 12. (a) Current signal of DC section (S1), (b) Output signal of FIS-1, (c) Phase A current signal of AC section (S2), (d) Output signal of FIS-2 for DC section (S1), and (e) Output signal of FIS-2 for section (S2) during fault (phase A-to-ground fault) in AC section against varying power angle (5°) with fault resistance of 1 Ω.

Table 8
Performance of the proposed method against different power angles.

Fault	Load angle/ Power angle	Fault Detection		Section Identification				Identification Result
		Trip logic output	Detection Time (ms)	Section 1		Section 2		
				Trip logic output	Identification Time (ms)	Trip logic output	Identification Time (ms)	
F1	5	1	3.34	0	-	1	5.67	Fault in AC side (S2)
	10	1	3.87	0	-	1	5.86	Fault in AC side (S2)
	15	1	4.45	0	-	1	4.93	Fault in AC side (S2)
F2	5	1	3.56	0	-	1	5.97	Fault in AC side (S2)
	10	1	4.65	0	-	1	6.34	Fault in AC side (S2)
	15	1	5.34	0	-	1	5.45	Fault in AC side (S2)
F3	5	1	4.67	0	-	1	5.76	Fault in AC side (S2)
	10	1	5.43	0	-	1	5.98	Fault in AC side (S2)
	15	1	4.98	0	-	1	6.77	Fault in AC side (S2)

Table 9
Performance of the proposed method against varying transmission line parameters.

Varying transmission line parameters	Fault Detection		Section Identification				Identification Result
	Trip logic output	Detection Time (ms)	Section 1		Section 2		
			Trip logic output	Identification Time (ms)	Trip logic output	Identification Time (ms)	
5%	1	0.42	1	3.19	0	–	Fault in DC side (S1)
−5%	1	0.45	1	3.75	0	–	Fault in DC side (S1)
10%	1	0.56	1	4.53	0	–	Fault in DC side (S1)
−10%	1	0.53	1	4.56	0	–	Fault in DC side (S1)
15%	1	0.76	1	5.38	0	–	Fault in DC side (S1)
−15%	1	0.73	1	5.76	0	–	Fault in DC side (S1)

Table 10
Performance of the proposed method against distortion in the signals.

Fault type	Location of the fault (km)	Distortion level SNR values in dB	Trip logic output	Detection Time (ms)
PP1G	5	30	1	4.56
		40	1	5.55
		50	1	6.57
	195	30	1	8.53
		40	1	8.55
		50	1	9.91
PP1NP2	5	30	1	5.67
		40	1	6.80
	195	30	1	9.57
		40	1	9.98

Performance of the method against varying transmission line parameters

The proposed method is tested by adjusting the parameters of the transmission line up to +15 percent in the presence of different types of faults. Table 9 illustrates the test results of the method during PG fault in section 1 with the change of transmission line parameters up to 15%. Simulated current waveforms for P1G fault at the rectifier end for section 1 and section 2 are shown in Fig. 13(a) and (c), respectively with varying line parameter (+5%) with fault resistance of 1 Ω. Fig. 13(b) highlights the output of the fault detection module and Fig. 13(d)-(e) shows the result of the faulty section identification module. As the fault happens in DC section with varying line parameter (+5%) and fault resistance of 1 Ω, the identification output of section S1 is 1 (fault condition) and the identification output of section 2 (S2) is 0 (no-fault), which is shown in Fig. 13(d)-(e). Thus, the proposed method detects the fault and identifies the fault section accurately during the variation in transmission line parameters.

Performance of the method against distortion in the signals

The performance of the proposed method against noise injected measurements under diverse signal-to-noise ratio (SNR) values is evaluated and the method detects all types of DC faults with an SNR of 30–50 dB. Table 10 integrates all the results.

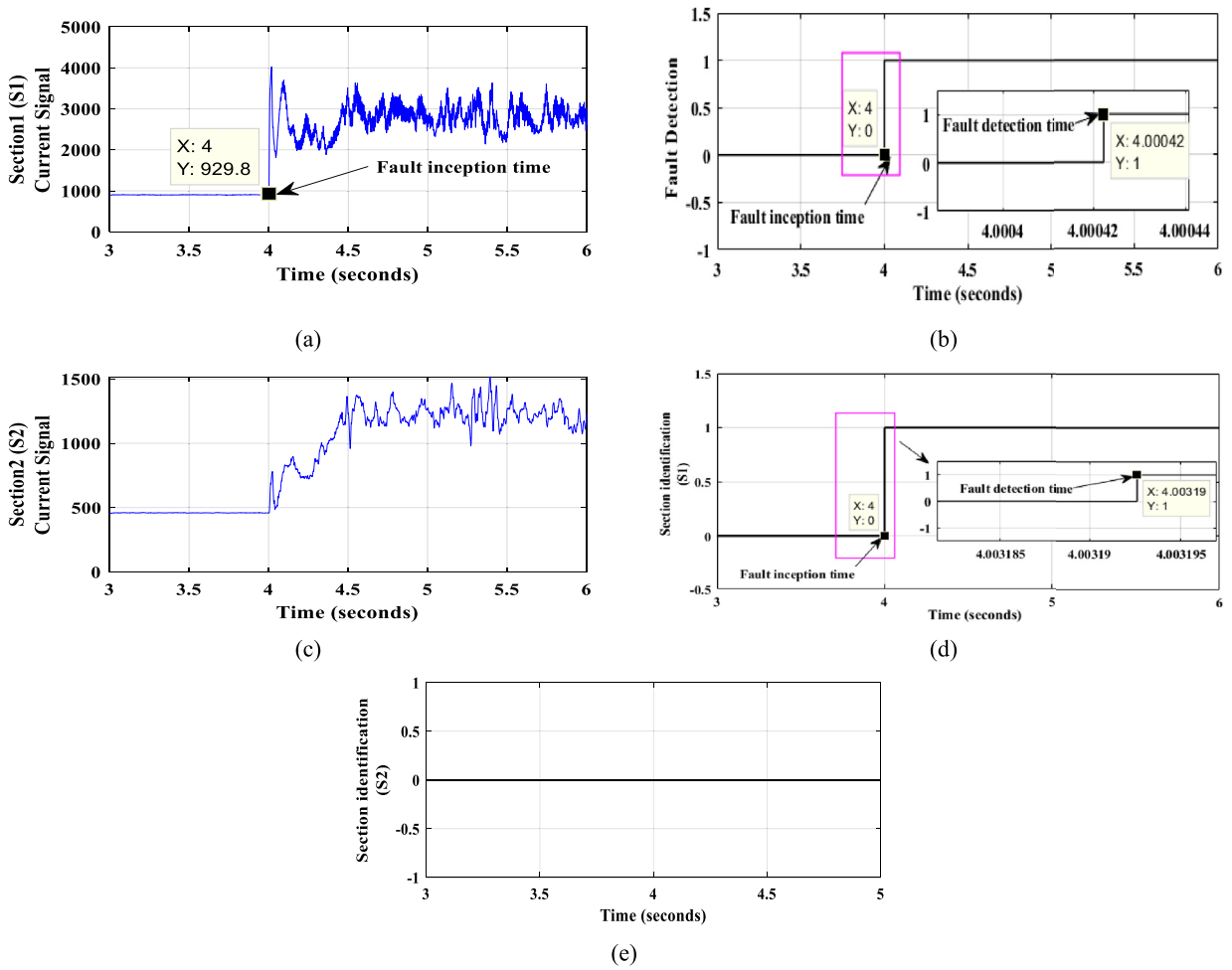

Fig. 13. (a) Current signal of DC section (S1), (b) Output of fault detection module, (c) Current signal of AC section (S2), (d) Output signal of FIS-2 for section (S1), and (e) Output signal of FIS-2 for section (S2) during fault in DC section with varying line parameter (+5%) and fault resistance of 1 Ω.

Comparison

This section makes a comparison between the proposed method and other existing method. Table 11 demonstrates how the strategies are compared in terms of technique used, input signal, sampling frequency, fault detection time, and accuracy. The proposed method accurately identifies faults such as far- and near-end faults, high variations in fault resistance as compared to other existing methods. The proposed method needs less sampling frequency and reach setting up to a line distance of 100 percent.

Conclusions and future scope

The FIS method with simple IF-THEN rules is used to recognize the fault in a VSC-based MT-HVDC model. The proposed method requires local current and voltage measurements consequently no telecommunication is required, resulting in low-cost as well as high reliability. The detailed test has been conducted to reassure the enhanced performance of the proposed method by considering different types of faults at specific fault positions, the influence of differing fault resistance, parameters of the transmission line, power angle, and existence of noise. The results of the simulation show that the proposed protection method detects the DC fault and appropriately identifies the faulty section. The method is also independent of the direction of power flow, include 100% reach setting of the relay, considering only one-end data, and small fault detection time (<1 ms) in most of the tested fault cases. Furthermore, the Fault section identification time is minimum 0.26 ms and maximum 9.98 ms. Thus, it is possible to promptly and accurately recognize and segregate against a DC fault with substantial short-circuit resistance. The suggested algorithm can be improved using new type-2 and type-3 fuzzy systems such as fault estimation for mode-dependent IT2 fuzzy systems with quantized output signals; optimal deep learning control for modernized microgrid etc.

Table 11
Comparison with existing schemes.

Methods	A Traveling-Wave-Based Methodology for Wide-Area Fault Location in Multi-terminal DC systems [5]	A Traveling-Wave-Based Fault Location Method for MMC-Based Multi-terminal DC Grids[24]	A differential protection technique for multi-terminal HVDC [29]	Wavelet-based protection strategy for DC faults in multi-terminal VSC HVDC systems [30]	A two-layer detection strategy for protecting multi-terminal HVDC systems against faults within a wide range of impedances [31]	Convolutional neural network based on fast Fourier transform and gramian angle field for fault identification of HVDC transmission line [32]	A novel time-domain method for fault detection and classification in VSC–HVDC transmission lines [33]	A waveform similarity-based protection scheme for the VSC–HVDC transmission lines [34]	Propos-ed method
Technique used	Traveling-wave-based methodology	Travelling wave-based methodology	Wavelet	Wavelet	A two-layer detection strategy	Fast Fourier transform, gramian angular field, and convolutional neural network	Intrinsic Time Decomposi-tion	Wavelet transform modulus maximum	Fuzzy Inference System
Sample of the HVDC system	VSC-based HVDC	MMC-based MT-HVDC	VSC-based HVDC	VSC-based HVDC	VSC-based HVDC	MMC-based MT-HVDC	VSC-based MT-HVDC	VSC- based HVDC	VSC-based MT-HVDC
Fault resistance	200	300	300	–	400	–	100	500	500
Signal taken	–	Bipole	Bipole	–	–	Bipole	Bipole	–	Monopole
Sampling frequency (kHz)	1000	1000	100	20	–	20	13.5	100	10
Fault identification time (ms)				5.25	>15	>1.5	<1.3	<1.12	Minimum 0.26 ms and max. 9.98ms
Accuracy (%)	–	–	–	100	–	100	–	–	100

Ethical approval

Not applicable.

CRediT authorship contribution statement

Upma Sahu: Conceptualization, Methodology, Software, Writing – original Draft, Writing – Review & Editing. **Anamika Yadav:** Conceptualization, Writing – Review & Editing, Supervision, Validation, Project administration. **Mohammad Pazoki:** Formal analysis, Review, Investigation and Supervision.

Availability of data and materials

Not applicable.

Declaration of Competing Interest

The authors declare that they have no known competing financial interests or personal relationships that could have appeared to influence the work reported in this paper.

Data availability

No data was used for the research described in the article.

Acknowledgments

This research did not receive any specific grant from funding agencies in the public, commercial, or not-for-profit sectors.

References

[1] U.N. Gnanarathna, A.M. Gole, R.P. Jayasinghe, Efficient modeling of modular multilevel HVDC converters (MMC) on electromagnetic transient simulation programs, IEEE Trans. Power Deliv. 26 (1) (2011) 316–324.
[2] N. Flourentzou, V.G. Agelidis, and G.D. Demetriades, “An overview VSC-based HVDC power transmission systems,” vol. 24, no. APRIL 2009, pp. 592–602, 2015.
[3] J. Beerten, S. Cole, R. Belmans, Generalized steady-state VSC MTDC model for sequential AC/DC power flow algorithms, IEEE Trans. Power Syst. 27 (2) (2012) 821–829.

[4] N.R. Chaudhuri, R. Majumder, B. Chaudhuri, J. Pan, Stability analysis of VSC MTDC grids connected to multimachine AC systems, IEEE Trans. Power Deliv. 26 (4) (2011) 2774–2784.
[5] S. Azizi, M. Sanaye-Pasand, M. Abedini, A. Hassani, A traveling-wave-based methodology for wide-area fault location in multiterminal DC systems, IEEE Trans. Power Deliv. 29 (6) (2014) 2552–2560.
[6] I. Jahn, N. Johannesson, S. Norrga, Survey of methods for selective DC fault detection in MTDC grids, IET Conf. Publ. 2017 (CP709) (2017) 1–7.
[7] P. Wang, Z. Li, X. Zhang, and P.F. Coventry, "Start-Up Sequences of an Offshore Integrated MMC MTDC System," pp. 1–7.
[8] B.K.J. Michael P.Bahrman, IEEE march/april 2007, Ieee Power Energy Mag (2007) 32–44 april.
[9] P. WANG, X.P. ZHANG, P.F. COVENTRY, Z. LI, Control and protection strategy for MMC MTDC system under converter-side AC fault during converter blocking failure, J. Mod. Power Syst. Clean Energy 2 (3) (2014) 272–281.
[10] X.P. Zhang, Multiterminal voltage-sourced converter-based HVDC models for power flow analysis, IEEE Trans. Power Syst. 19 (4) (2004) 1877–1884.
[11] D. Van Hertem, M. Ghandhari, Multi-terminal VSC HVDC for the European supergrid : obstacles, Renew. Sustain. Energy Rev. 14 (9) (2010) 3156–3163.
[12] W. Lu, B.T. Ooi, Multi-terminal HVDC as enabling technology of premium quality power park, Proc. IEEE Power Eng. Soc. Transm. Distrib. Conf. 2 (1) (2002) 719–724.
[13] M. Dodangeh and N. Ghaffarzadeh, "A new fast and accurate fault location and classification method on MTDC microgrids using current injection technique, traveling-waves, Online Wavelet, and Mathematical Morphology."
[14] J.G. Ciezki, R.W. Ashton, Selection and stability issues associated with a navy shipboard DC Zonal Electric Distribution System, IEEE Trans. Power Deliv. 15 (2) (2000) 665–669.
[15] R. Marquardt, Modular multilevel converter: an universal concept for HVDC-networks and extended DC-bus-applications, in: 2010 Int. Power Electron. Conf. - ECCE Asia -, IPEC 2010, 2010, pp. 502–507.
[16] L. Livermore, J. Liang, J. Ekanayake, MTDC VSC technology and its applications for wind power, in: Proc. Univ. Power Eng. Conf, 2010, pp. 1–6.
[17] A. Torralba, J. Chavez, L.G. Franquelo, Fault detection and classification of analog circuits by means of fuzzy logic-based techniques, in: Proc. - IEEE Int. Symp. Circuits Syst, 3, 1995, pp. 1828–1831.
[18] J.M. Johnson, A. Yadav, Complete protection scheme for fault detection, classification and location estimation in HVDC transmission lines using support vector machines, IET Sci. Meas. Technol. 11 (3) (2017) 279–287.
[19] V. Ashok, A. Yadav, A.Y. Abdelaziz, MODWT-based fault detection and classification scheme for cross-country and evolving faults, Electr. Power Syst. Res. 175 (2019) 105897 June.
[20] J. Moshtagh, M. Jannati, H.R. Baghaee, E. Nasr, A novel approach for online fault detection in HVDC converters, in: 2008 12th Int. Middle East Power Syst. Conf. MEPCON 2008, 2008, pp. 307–311.
[21] A.S. Silva, R.C. Santos, J.A. Torres, D.V. Coury, An accurate method for fault location in HVDC systems based on pattern recognition of DC voltage signals, Electr. Power Syst. Res. 170 (2018) 64–71 December2019.
[22] D. Tzelepis, G. Fusiek, A. Dysko, P. Niewczas, C. Booth, X. Dong, Novel fault location in MTDC grids with non-homogeneous transmission lines utilizing distributed current sensing technology, IEEE Trans. Smart Grid 9 (5) (2018) 5432–5443.
[23] S. Agarwal, A. Swetapadma, C. Panigrahi, A. Dasgupta, A method for fault section identification in High voltage direct current transmission lines using one End measurements, Electr. Power Syst. Res. 172 (2017) 140–151 December2019.
[24] S. Zhang, G. Zou, Q. Huang, H. Gao, A traveling-wave-based fault location scheme for MMC-based multi-terminal DC grids, Energies 11 (2) (2018).
[25] U. Sahu, A. Yadav, Fault detection in MTDC network utilising one end measurements, 2019 8th Int. Conf. Power Syst. Transit. Towar. Sustain. Smart Flex. Grids, ICPS, 2019, 2019.
[26] A. Hadaeghi, H. Samet, T. Ghanbari, Multi extreme learning machine approach for fault location in multi-terminal high-voltage direct current systems, Comput. Electr. Eng. 78 (2019) 313–327.
[27] Silvano Casoria, (Hydro-Quebec), VSC-based transmission system (Detailed model), Matlab documentation, Matlab (2018).
[28] S. Xue, J. Lian, J. Qi, B. Fan, Pole-to-ground fault analysis and fast protection scheme for HVDC based on overhead transmission lines, Energies 10 (7) (2017).
[29] A.E.B. Abu-Elanien, A.A. Elserougi, A.S. Abdel-Khalik, A.M. Massoud, S. Ahmed, A differential protection technique for multi-terminal HVDC, Electr. Power Syst. Res. 130 (2016) 78–88.
[30] K. De Kerf, et al., Wavelet-based protection strategy for DC faults in multi-terminal VSC HVDC systems, IET Gener. Transm. Distrib. 5 (4) (2011) 496–503.
[31] J.I. Marvik, S. D'Arco, J.A. Suul, A two-layer detection strategy for protecting multi-terminal HVDC systems against faults within a wide range of impedances, IET Conf. Publ. 2016 (CP671) (2016) 1–6.
[32] Can Ding, Zhenyi Wang, Qingchang Ding, Zhao Yuan, Convolutional neural network based on fast Fourier transform and gramian angle field for fault identification of HVDC transmission line, Sustain. Energy, Grid. Netw. 32 (2022) 100888.
[33] Amir Imani, Zahra Moravej, Mohammad Pazoki, A novel time-domain method for fault detection and classification in VSC-HVDC transmission lines, Int. J. Electr. Power Energy Syst. 140 (2022) 108056.
[34] Yuhan Zhang, Shunliang Wang, Tianqi Liu, A waveform-similarity-based protection scheme for the VSC-HVDC transmission lines, Int. J. Electr. Power Energy Syst. 144 (2023) 108571.